

# Technical Note: Revisiting the Procedure for Quantification of the Young Water Fraction Based on Seasonal Tracer Cycles

Tam V. Nguyen<sup>1</sup>, Rohini Kumar<sup>2</sup>, Ingo Heidbüchel<sup>1,3</sup>, Arianna Borriero<sup>1</sup>, Jan H. Fleckenstein<sup>1,3</sup>

<sup>1</sup>Department of Hydrogeology, Helmholtz Centre for Environmental Research - UFZ, Leipzig, Germany.

<sup>2</sup>Department of Computational Hydrosystems, Helmholtz Centre for Environmental Research - UFZ, Leipzig, Germany.

<sup>3</sup>Bayreuth Centre of Ecology and Environmental Research, University of Bayreuth, Bayreuth, Germany.

Corresponding author: Tam V. Nguyen ([tam.nguyen@ufz.de](mailto:tam.nguyen@ufz.de))

## Key Points:

- We propose an alternative procedure to estimate the young water fraction with any given age threshold
- The estimated young water fractions from the traditional and proposed procedures can be substantially different
- The estimated young water fraction increases significantly when the isotope sampling frequency changes from submonthly to monthly time steps

**Abstract**

The transit time (TT) of streamflow encapsulates information about how catchments store and release water and solutes of different ages. The young water fraction ( $F_{yw}$ ), the fraction of streamflow that is younger than a certain age (normally 2–3 months), has been increasingly used as an alternative metric to the commonly used mean TT (mTT). In the commonly used ('traditional') procedure presented by Kirchner (2016), the age threshold ( $\tau_{yw}$ ) of  $F_{yw}$  separating young from old water is not pre-defined and differs from catchment to catchment depending on the shape of the (gamma) transit time distribution. However, it can be argued that it is important to use the same pre-defined  $\tau_{yw}$  for inter-catchment comparison of  $F_{yw}$ . In this study, we propose an alternative ('proposed') procedure for the estimation of  $F_{yw}$  with any pre-defined  $\tau_{yw}$ . This allows us to also compare the effects of data sampling frequencies on the results of  $F_{yw}$  estimation using the same  $\tau_{yw}$ . We applied the traditional and proposed procedures using daily oxygen isotope ( $\delta^{18}\text{O}$ ) data in the Alp and Erlenbach catchments, Switzerland. We found that our proposed and the traditional procedure can give very different  $F_{yw}$  values. With the proposed procedure, the estimated  $F_{yw}$  significantly increases when the sampling frequency changes from sub-monthly to monthly time steps. Overall, our study highlights the importance of the selection of  $\tau_{yw}$  and the sampling frequency in  $F_{yw}$  estimation, which should be given more attention.

## 1 Introduction

The transit time (TT) of streamflow, the time between a water parcel entering a catchment as precipitation and exiting as streamflow at the catchment outlet, is an important descriptor for understanding how catchments store and release water and solutes (McGuire & McDonnell, 2006). TT can be incorporated into water quality models to estimate the time origin of water and solutes in streamflow (Hrachowitz et al., 2016; Nguyen et al., 2021; Nguyen et al., 2022), thus providing useful implications for water quality management and vulnerability assessment. In recent years, the young water fraction ( $F_{yw}$ ), the fraction of streamflow that is younger than a specific age threshold ( $\tau_{yw}$ ), typically around 2-3 months (Kirchner, 2016), has been emerging as an alternative metric of the TT distribution (TTD) of catchments compared to the often used mean TT (mTT). The use of  $F_{yw}$  has gained momentum because it can be derived robustly and with much higher accuracy than the mTT at the catchment scale even from coarse and irregular tracer sampling frequencies or under conditions of spatial heterogeneity (Kirchner, 2016). The young water fraction has been used from local and regional (Burt et al., 2022; Lutz et al., 2018; Song et al., 2017; von Freyberg et al., 2018) to global (Jasechko et al., 2016) scales. In these studies,  $F_{yw}$  is often used for inter-catchment comparisons to shed light on the underlying hydrological functioning of different catchments.

One of the challenges when using  $F_{yw}$  estimated from the seasonal tracer concentrations in precipitation and streamflow using the procedure proposed by Kirchner (2016) is that the estimated  $\tau_{yw}$  will vary between catchments depending on the actual shape of the TTD. Still, the actual  $\tau_{yw}$  values are often not reported in inter-catchment comparisons using  $F_{yw}$  (Gallart, von Freyberg, et al., 2020; Lutz et al., 2018; von Freyberg et al., 2018). Therefore, it is unclear how we can evaluate the effects of climate and catchment properties on  $F_{yw}$  among catchments if they correspond to different  $\tau_{yw}$  values. This is because differences in  $F_{yw}$  among catchments can either be driven by climate factors and physical characteristics of the catchment or different  $\tau_{yw}$  values. Therefore, it would be highly beneficial to use the same  $\tau_{yw}$  when comparing  $F_{yw}$  among catchments. Alternatively,  $\tau_{yw}$  could also be a user-defined (but fixed) parameter, allowing  $F_{yw}$  calculation for any given  $\tau_{yw}$  (e.g., 7, 75, or 365 days; Benettin et al., 2020), depending on the hydrological/water quality process of interest.

Varying tracer sampling frequencies are another potential source of inaccuracy in the comparison of  $F_{yw}$  across various catchments. While  $F_{yw}$  can be estimated with coarse and irregular tracer sampling frequencies spanning over multiple years (e.g., at least 2-3 years; Benettin et al., 2022), it is unclear how the tracer sampling frequency affects the estimated  $F_{yw}$ , especially when the same  $\tau_{yw}$  is considered. Stockinger et al. (2016) found that the estimated  $F_{yw}$  increases almost two-fold with a high sampling frequency (daily and sub-daily) compared to that of weekly sampling frequency. Gallart, Valiente, et al. (2020) also found that the estimated  $F_{yw}$  at weekly sampling frequency is significantly lower than that of dynamic sampling (sub-weekly with variable time steps). However, in these studies,  $F_{yw}$  estimated with different sampling frequencies corresponds to different  $\tau_{yw}$ . Stockinger et al. (2016) suggested considering the role of isotope sampling frequency in inter-catchment comparisons based on  $F_{yw}$ . Based on these insights, we see the need to conduct such a study using a fixed  $\tau_{yw}$  for  $F_{yw}$ .

The objective of this study is to propose an alternative procedure for estimating  $F_{yw}$  based on seasonal tracer cycles in precipitation and streamflow proposed by Kirchner (2016). Here, we (a) propose a more direct procedure, allowing  $F_{yw}$  to be estimated with any user-defined  $\tau_{yw}$ , and (b) evaluate the effect of tracer sampling frequencies on the estimated  $F_{yw}$  with a fixed  $\tau_{yw}$ . To

this end, we used high-frequency tracer (isotope) data from the Alp catchment and one of its tributaries (Freyberg et al., 2022).

## 2 Materials and Methods

### 2.1 Study area and data

We selected the Alp catchment (47 km<sup>2</sup>) and one of its tributary catchments (i.e., the Erlenbach, 0.7 km<sup>2</sup>; Fig. 1a) of which high-frequency stable isotopes of hydrogen ( $\delta^2\text{H}$ ) and oxygen ( $\delta^{18}\text{O}$ ) in precipitation and streamflow and hydro-meteorological data are publicly available (Freyberg et al., 2022). The elevation of the Alp catchment ranges from 840 to 1896 m above sea level (a.s.l) while that of the Erlenbach catchment spans from 1,111 to 1,654 m a.s.l. The average annual average precipitation in the Alp and Erlenbach catchments amounts to about 1413 and 1,625 mm/year, respectively. The runoff coefficient (streamflow divided by precipitation) of the Alp is 93% while that of the Erlenbach is 70% (derived from data from Freyberg et al. (2022)). The hydro-climatic regime of both catchments is classified as a hybrid catchment (i.e., streamflow affected by both rainfall and snow (Staudinger et al., 2017; Von Freyberg et al., 2018)).

In this study, we only used oxygen-18 isotope ( $\delta^{18}\text{O}$ ) data because of its high correlation with deuterium isotope ( $\delta^2\text{H}$ ) (von Freyberg et al., 2022) and a negligible evaporation-induced fractionation of  $\delta^{18}\text{O}$  (Lutz et al., 2018). In both catchments, the  $\delta^{18}\text{O}$  values in streamflow vary

in a much narrower range compared to the ones in precipitation (Fig. 1b-c). More information about the study area as well as the data can be found in Freyberg et al. (2022).

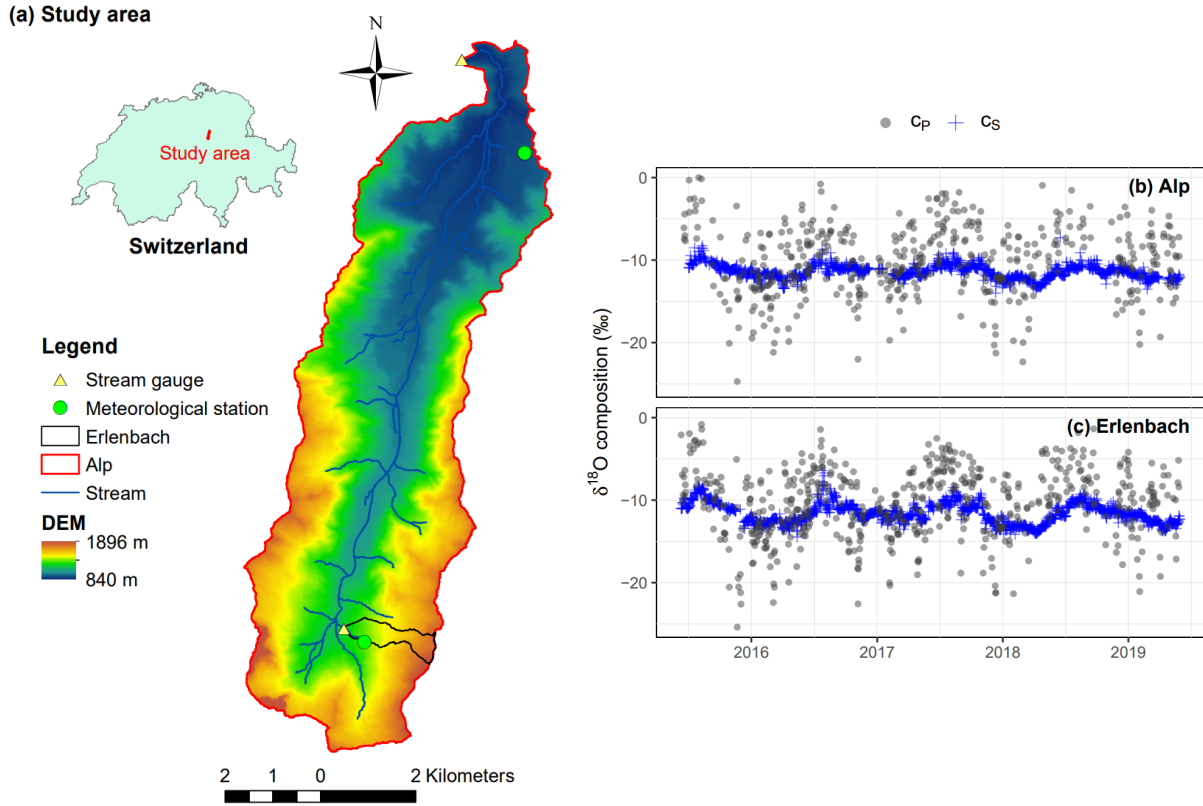


**Figure 1.** (a) Location and digital elevation model (DEM) of the Alp and Erlenbach catchments along with observed  $\delta^{18}\text{O}$  composition of precipitation ( $c_p$ ) and streamflow ( $c_s$ ) in the (b) Alp and (c) Erlenbach catchments.

## 2.2 Theoretical background

The approach for estimating the young water fraction ( $F_{yw}$ ) from seasonal tracer (e.g., stable isotopes of oxygen and hydrogen) cycles (Kirchner, 2016) in precipitation and streamflow assumes that the catchment is in a steady state, and that the transit time distribution (TTD) is time-invariant. While TTDs can have very different shapes, here we focus on a family of gamma distributions of the following form:

$$h(\tau) = \frac{\tau^{\alpha-1}}{\beta^\alpha \Gamma(\alpha)} e^{-\tau/\beta} \quad (1)$$

where  $h(\tau)$  (-) is the gamma function (in the form of a probability density distribution function) with shape factor  $\alpha$ , scale factor  $\beta$ , and transit time  $\tau$ . The tracer concentration in precipitation,  $c_p(t)$ , is assumed to follow the sine wave function throughout the year:

$$c_p(t) = A_p \sin(2\pi f t - \varphi_p) + k_p \quad (2)$$

where  $A_p$  is the amplitude,  $f$  is the frequency of the cycle ( $f = 1 \text{ year}^{-1}$  for annual cycle),  $\varphi_p$  is the phase of the tracer cycle in precipitation (ranging from  $[0, 2\pi]$ , corresponding to the start and

the end of a calendar year),  $k_p$  is the average tracer concentration in precipitation, and the subscript “P” refers to precipitation.

The tracer concentration in streamflow,  $c_s(t)$ , is given by the convolution of the forward TTDs (Eq. 1) with tracer concentration in precipitation  $c_p(t)$  (Eq. 2), ignoring the effect of evaporative fractionation (Kirchner, 2016):

$$c_s(t) = \int_{\tau=0}^{\tau=\infty} h(\tau) \cdot c_p(t - \tau) \cdot d\tau \quad (3)$$

where  $c_p(t - \tau)$  is the tracer concentration in precipitation at time  $t - \tau$ , and the subscript “S” refers to streamflow.  $F_{yw}$  can be estimated using the regularized lower incomplete gamma function (Eq. 1), as shown below:

$$F_{yw} = \int_{\tau=0}^{\tau=\tau_{yw}} \frac{\tau^{\alpha-1}}{\beta^\alpha \Gamma(\alpha)} \cdot e^{-\tau/\beta} \cdot d\tau \quad (4)$$

### 2.3. Traditional procedure for $F_{yw}$ estimation from Kirchner (2016)

The **first step** is to fit the sine wave (Eq. (2) or its revised form, Eq. (5), as shown below) to observed tracer concentrations in precipitation (Kirchner, 2016; Lutz et al., 2018; Stockinger et al., 2016; von Freyberg et al., 2018). The fitted sine wave is often in the form of a linear function between  $c_p(t)$  and parameters that are needed to be estimated, as shown below:

$$\begin{aligned} c_p(t) &= A_p \sin(2\pi f t - \varphi_p) + k_p \\ &= A_p \sin(2\pi f t) \cdot \cos(\varphi_p) - A_p \cos(2\pi f t) \cdot \sin(\varphi_p) + k_p \\ &= -A_p \cdot \sin(\varphi_p) \cdot \cos(2\pi f t) + A_p \cdot \cos(\varphi_p) \cdot \sin(2\pi f t) + k_p \\ &= a_p \cdot \cos(2\pi f t) + b_p \cdot \sin(2\pi f t) + k_p \end{aligned} \quad (5)$$

where

$$a_p = -A_p \cdot \sin(\varphi_p) \quad (6)$$

$$b_p = A_p \cdot \cos(\varphi_p) \quad (7)$$

$$a_p^2 + b_p^2 = A_p^2 \cdot \sin^2(\varphi_p) + A_p^2 \cdot \cos^2(\varphi_p) = A_p^2 \quad (8)$$

$$\frac{a_p}{b_p} = \frac{-A_p \cdot \sin(\varphi_p)}{A_p \cdot \cos(\varphi_p)} = -\tan(\varphi_p) \quad (9)$$

$$\varphi_p = \arctan(-a_p/b_p) \quad (10)$$

The parameters ( $a_p$ ,  $b_p$  and  $k_p$ ) can be estimated based on observed tracer concentration in precipitation using the iteratively least squares (IRLS) regression approach which can limit the effect of outliers in observed data. Equation (10) presented here differs from the one given by Kirchner (2016) ( $\varphi_p = \arctan(b_p/a_p)$ ), which we suppose is due to a typo in the Kirchner (2016) work. Equation (10) always give two values of  $\varphi_p$  within the range of  $[0, 2\pi]$  as  $\tan(\varphi_p) = \tan(\varphi_p \pm \pi)$ , the correct value of  $\varphi_p$  could be selected using Eqs. (6-7).

The **second step** is to fit the sine wave (Eq. (11) or (12)) to the observed tracer concentration in streamflow (Kirchner, 2016; Lutz et al., 2018; Freyberg et al., 2018). This is because convolutions (Eq. 3) are linear operators and, therefore, transform the sine wave input signal (Eq. 2) into a sine wave output signal with a phase shift and damped amplitude due to

mixing and dispersion processes within the catchment (Kirchner, 2016). It can be expressed in the following form:

$$c_S(t) = A_S \sin(2\pi ft - \varphi_S) + k_S \quad (11)$$

where  $A_S$ ,  $\varphi_S$ , and  $k_S$  are the amplitude, phase, and average tracer concentration in streamflow, respectively. Similar to Eq. (5), Eq. (11) can be rewritten as follows:

$$c_S(t) = a_S \cdot \cos(2\pi ft) + b_S \cdot \sin(2\pi ft) + k_S \quad (12)$$

with

$$a_S = -A_S \cdot \sin(\varphi_S) \quad (13)$$

$$b_S = A_S \cdot \cos(\varphi_S) \quad (14)$$

$$a_S^2 + b_S^2 = A_S^2 \cdot \sin^2(\varphi_S) + A_S^2 \cdot \cos^2(\varphi_S) = A_S^2 \quad (15)$$

$$\varphi_S = \arctan(-a_S/b_S) \quad (16)$$

Due to the delay in the tracer concentration signal from rainfall to streamflow when it travels through the catchment,  $\varphi_S$  must be greater than  $\varphi_P$ . With the yearly tracer cycle,  $\varphi_S - \varphi_P$  must be within the range of  $[0, 2\pi)$ .

The **third step** is to find  $F_{yw}$ . Kirchner (2016) demonstrated that the amplitude ratio ( $A_S/A_P$ ) approximates  $F_{yw}$  and is free from aggregation bias, therefore, this ratio is used to estimate  $F_{yw}$ :

$$F_{yw} \approx \frac{A_S}{A_P} \quad (17)$$

The amplitude ratio ( $A_S/A_P$ ) is controlled by the shape  $\alpha$  and scale  $\beta$  factors of the gamma TTD since the tracer concentration in streamflow is a convolution of the tracer concentration in precipitation with the gamma TTD (Eq. (3)):

$$\frac{A_S}{A_P} = (1 + (2\pi f\beta)^2)^{-\alpha/2} \quad (18)$$

From Eqs. (4), (17), and (18), we have:

$$(1 + (2\pi f\beta)^2)^{-\alpha/2} \approx \int_{\tau=0}^{\tau=\tau_{yw}} \frac{\tau^{\alpha-1}}{\beta^\alpha \Gamma(\alpha)} \cdot e^{-\tau/\beta} \cdot d\tau \quad (19)$$

Kirchner (2016) then numerically searched for the  $\tau_{yw}$  which makes the left- and right-hand sides of Eq. (19) approximately equal. If  $\alpha$  and  $\beta$  are within the range of  $[0.2, 2]$  and  $[0, \infty)$ ,

respectively,  $\tau_{yw}$  can be estimated using the following approximation with a root mean square difference between the left- and right-hand sides of Eq. (19) of less than 2.3% (Kirchner, 2016):

$$\tau_{yw}/T \approx 0.0949 + 0.1065\alpha - 0.0126\alpha^2 \quad (20)$$

where  $T = 1$  (year) for the annual tracer cycle.

Parameters ( $\alpha$  and  $\beta$ ) of the gamma TTD can be calculated from the phase shift and amplitude ratio of the fitted sine waves of the tracer concentrations in streamflow and precipitation as follows (Kirchner, 2016):

$$\varphi_S - \varphi_P = \alpha \cdot \arctan \left( \sqrt{(A_S/A_P)^{-2/\alpha} - 1} \right) \quad (21)$$

$$\beta = \frac{1}{2\pi f} \sqrt{(A_S/A_P)^{-2/\alpha} - 1} \quad (22)$$

#### 2.4. Proposed procedure for $F_{yw}$ estimation

Here, we propose an alternative procedure for  $F_{yw}$  estimation, as described in the following steps:

- **Step 1:** Fit the sine wave function (Eq. (2)) to the observed tracer concentration in precipitation to obtain a sine wave input signal.
- **Step 2:** Adjust the transfer function (Eq. 3) so that the convolution results in a sine wave function that represents the observed tracer concentration in streamflow to find the shape ( $\alpha$ ) and scale ( $\beta$ ) parameters of the gamma TTD.
- **Step 3:** Estimate  $F_{yw}$  directly from the fitted gamma TTD with any given age threshold  $\tau_{yw}$  using Eq. (4).

Steps 1 and 2 can be done with any non-linear fitting or optimization techniques. As an example, we propose a simple approach for fitting these non-linear functions to observed data and for quantifying associated parameter uncertainty. In step 1, we first define the range for the parameters ( $A_P$ ,  $\varphi_P$ ,  $k_P$ ) of the sine wave function, which can be roughly estimated based on the observed seasonal tracer concentration in precipitation. Then, we randomly sample different parameter sets (within their respective ranges) using uniform Latin Hypercube Sampling (LHS). The best (or list of behavioral) parameter set(s) can be selected based on the (weighted) mean square error (MSE), depending on the estimated  $F_{yw}$  (weighted or unweighted). The weights for the MSE can, for example, be the precipitation volumes. This approach could be used for estimating parameters ( $\alpha$ ,  $\beta$ ) of the gamma distribution in step 2. Here, we generate a number of parameter sets for the gamma distribution using LHS; then we randomly combine them with the behavioral parameter sets of the sine wave function found in step 1. The best (or behavioral) parameter set(s) of the gamma function can be selected based on a given error measure (e.g., MSE) estimated between simulated and observed instream tracer concentrations. The mean square error can be weighted by discharge volume to get the weighted  $F_{yw}$ . The uncertainty in the estimated  $F_{yw}$  can be quantified from behavioral parameter sets of the gamma function.

#### 2.5. Experimental design

We first compare the estimated  $F_{yw}$  from the traditional and proposed procedures for both catchments. In this experiment, the original high-frequency  $\delta^{18}\text{O}$  data are used. As the original and proposed procedures are similar in the first step, we use the same best-fit sine wave function

to observed  $\delta^{18}\text{O}$  composition in precipitation for the traditional and proposed procedure. For the proposed procedure, we then use the 100 best-fit gamma functions and calculate  $F_{yw}$  with the  $\tau_{yw}$  found from the traditional procedure to account for parameter uncertainty. With the traditional procedure, we only used the best-fit sine wave function when fitting to observed  $\delta^{18}\text{O}$  composition in streamflow as the uncertainty in this method does not correspond to the same  $\tau_{yw}$  value.

In the second experiment, we evaluate the effect of data sampling frequency on the estimated young water fraction using our proposed procedure. To have continuous daily data (isotope, precipitation, and streamflow), we interpolated missing values using the linear (in time) interpolation technique with the “*approx*” function in R (R Core Team, 2021). Then, we sample the data at weekly (7 days), bi-weekly (14 days), and monthly (30 days) intervals with a random starting date. The dates of sampling are the same for precipitation, isotope, and streamflow data to maintain their temporal consistency. The thresholds of  $\tau_{yw}$  are set as 2 months (0.164 years) and 3 months (0.246 years) (e.g., Kirchner, 2016; Lutz et al., 2018; Song et al., 2017; Von Freyberg et al., 2018).

The (weighted)  $F_{yw}$  values calculated from the above experiments have often been used in previous studies (Lutz et al., 2018; Stockinger et al., 2016; von Freyberg et al., 2018). Here, we consider snowpack storage as part of the catchment storage (e.g., Jasechko et al., 2016; Song et al., 2017); in other words, we do not distinguish between precipitation in liquid and snow form since differentiating them has almost no effect on the estimated  $F_{yw}$  (Freyberg et al., 2018).

### 3 Results

#### 3.1. Traditional versus proposed procedures

Figure 2(a-b) shows that the fitted sine waves to the observed  $\delta^{18}\text{O}$  in precipitation from the traditional and proposed procedures for the two catchments only have minor differences, which is also shown by their similarity in the amplitude ( $A_P$ ), the average  $\delta^{18}\text{O}$  ( $k_P$ ), and the phase ( $\phi_P$ ) (Table 1). In the traditional procedure, the fitted sine wave is in theory the one with the lowest weighted MSE as linear regression is used in this procedure (Su et al., 2012). In the

proposed procedure, the fitted sine wave will be similar to the ones from the traditional approach when the number of parameter sets sampled by LHS is large.

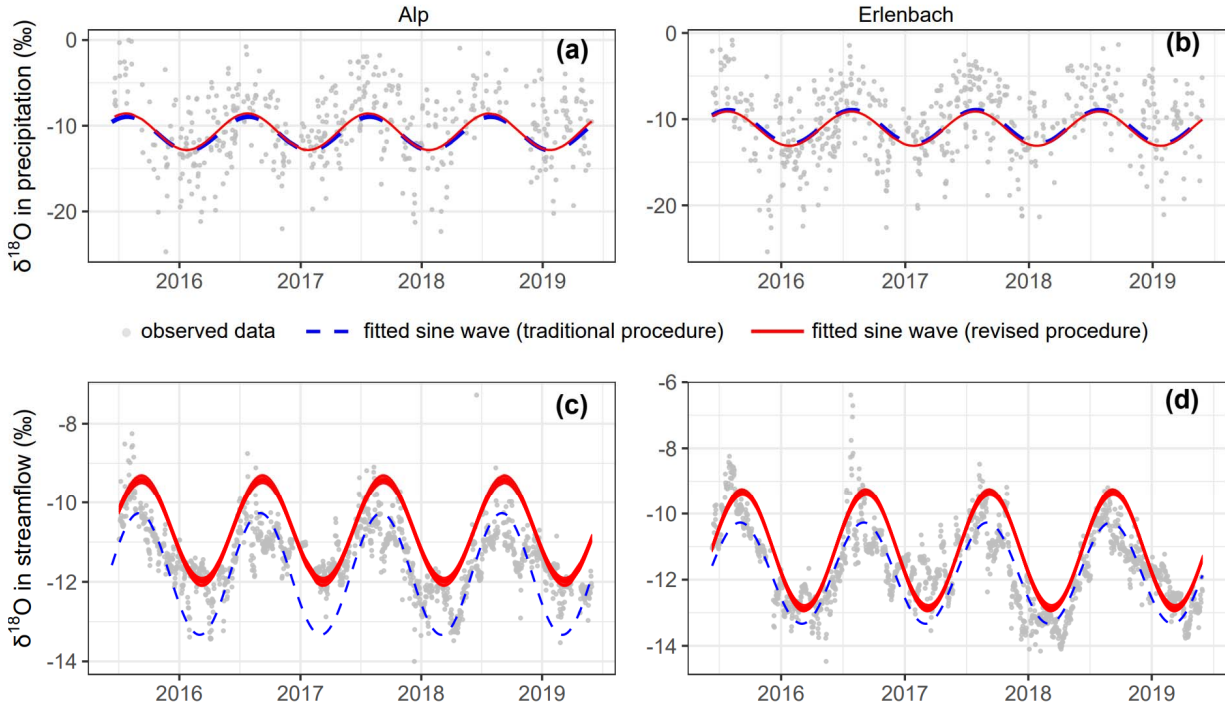


**Figure 2.** Observed and fitted sine wave to  $\delta^{18}\text{O}$  in precipitation (a, b) and  $\delta^{18}\text{O}$  in streamflow (c, d) from (a, c) the Alp and (b, d) the Erlenbach catchments with the traditional and proposed procedures. In the traditional approach, only the best-fit sine wave to  $\delta^{18}\text{O}$  in precipitation the best-fit sine wave to  $\delta^{18}\text{O}$  in streamflow is used. In the proposed procedure, the best-fit sine wave to  $\delta^{18}\text{O}$  to precipitation and the 100 best-fit sine waves to  $\delta^{18}\text{O}$  in streamflow (derived from the convolution of the input sine wave and the gamma functions) are used.

The sine wave that is fitted directly to the observed  $\delta^{18}\text{O}$  in streamflow from the traditional procedure has a better fit compared to the fitted sine waves derived from the convolution of the input sine wave via a gamma distribution from the proposed procedure (Figure 2c-d). This is expected because the sine wave fitted directly to  $\delta^{18}\text{O}$ s in streamflow from the traditional procedure is not constrained by mass conservation. In other words, the mean  $\delta^{18}\text{O}$  in precipitation equals the mean  $\delta^{18}\text{O}$  in streamflow from the proposed procedure. However, they are not exactly equal to the observed data (e.g., Alp catchment:  $k_P = -10.581\text{‰}$ ,  $k_S = -11.507\text{‰}$ ; Erlenbach catchment:  $k_P = -10.921\text{‰}$ ,  $k_S = -11.802\text{‰}$ ; Table 1) due to uncertainty in observed data, or the time series data are not sufficiently long, or unaccounted processes. As a result, the observed  $\delta^{18}\text{O}$  in streamflow is systematically overestimated in the proposed procedure. In this case, parameters of the gamma distribution cannot be inferred precisely from the sine waves fitted directly to the observed  $\delta^{18}\text{O}$  in precipitation and streamflow from the traditional procedure as Eq. (3) is violated. In that sense, the errors in the estimated  $F_{yw}$  could be much larger than the random errors in the observed  $\delta^{18}\text{O}$  data (Kirchner, 2016). In fact,  $\delta^{18}\text{O}$  in streamflow calculated

by convolving the gamma function found from the traditional procedure with the sine wave input signals does not fit better (larger weighted MSE) than the ones from the proposed procedure.

**Table 1.** The estimated young water fractions and other parameters from the traditional and proposed procedures for the two test catchments. Numbers in subscripts indicate the equations used for the estimation of these values. In the proposed procedure, the  $\alpha$ ,  $\beta$ , and  $F_{yw}$  values are reported as the mean (numbers outside the brackets) and interquartile range (numbers inside the brackets) from the 100 best-fit gamma distributions.

Parameters	Alp		Erlenbach	
	Traditional procedure	Proposed procedure	Traditional procedure	Proposed procedure
$A_P$ (‰)	2.186 <sup>(8)</sup>	2.134	1.972 <sup>(8)</sup>	1.991
$\phi_P$ (rad)	1.947 <sup>(6,7,10)</sup>	1.946	2.017 <sup>(6,7,10)</sup>	1.977
$k_P$ (‰)	-10.581	-10.699	-10.921	-11.100
$A_S$ (‰)	0.971 <sup>(15)</sup>	not defined	1.530 <sup>(15)</sup>	not defined
$\phi_S$ (rad)	2.698 <sup>(13,14,16)</sup>	not defined	2.626 <sup>(13,14,16)</sup>	not defined
$k_S$ (‰)	-11.507	not defined	-11.802	not defined
$\phi_S - \phi_B$ (rad)	0.751	not defined	0.609	not defined
$\alpha$ (-)	0.564 <sup>(21)</sup>	0.802 [0.740, 0.906]	0.813 <sup>(21)</sup>	2.708 [2.170, 3.695]
$\beta$ (years)	0.650 <sup>(22)</sup>	0.246 [0.212, 0.285]	0.148 <sup>(22)</sup>	0.046 [0.034, 0.058]
$\tau_{yw}$ (years)	0.151 <sup>(20)</sup>	0.151 (user-defined)	0.173 <sup>(20)</sup>	0.173 (user-defined)
$F_{yw}$	0.444 <sup>(17)</sup>	0.556 [0.539, 0.576]	0.775 <sup>(17)</sup>	0.779 [0.744, 0.803]

In this study, the estimated parameters of the gamma TTDs from the traditional procedure are outside the interquartile ranges determined by the proposed procedure, resulting in different  $F_{yw}$ , especially in the Alp catchment (Table 1 and Figure 3a-b). In the Erlenbach catchment, despite discrepancies between the estimated parameters from the traditional and proposed procedures, the estimated  $F_{yw}$  from the traditional procedure is similar to the mean  $F_{yw}$  found from the proposed procedure (Figure 3b). However, if other age thresholds are used, there could be a large difference in the estimated  $F_{yw}$  from the two procedures as the parameters of the TTD

from these procedures are substantially different (e.g., if  $\tau_{yw} = 0.22$  years, then  $F_{yw} = 0.83$  (given  $\alpha = 0.813$  and  $\beta = 0.148$ ),  $F_{yw} = 0.94$  (given  $\alpha = 2.170$  and  $\beta = 0.046$ ), Eq. (4)) .

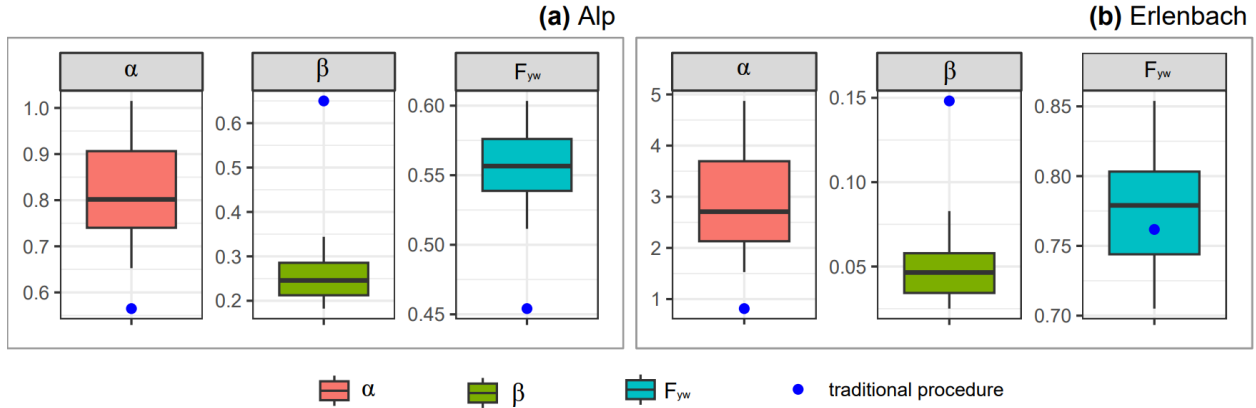
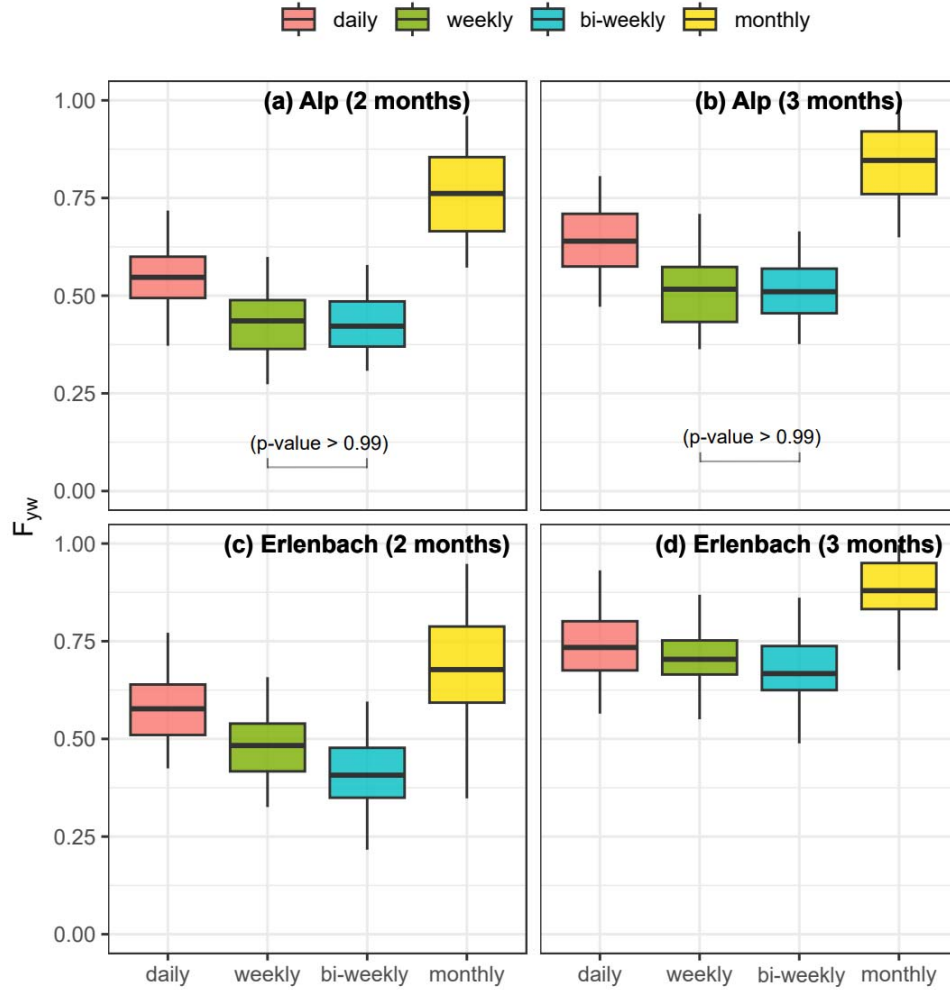


**Figure 3.** Parameters of the gamma function ( $\alpha$  and  $\beta$ ) and young water fraction ( $F_{yw}$ ) estimated from the traditional (blue point) and proposed procedure (boxplots) for (a) the Alp and (b) the Erlenbach catchments.

### 3.2. Effect of data sampling frequency on $F_{yw}$ estimation

Figure 4 shows the effect of data sampling frequency on the estimated  $F_{yw}$  (with  $\tau_{yw}$  of 2 and 3 months) for the Alp and Erlenbach catchments. In most cases, the differences in the mean  $F_{yw}$  from different sampling frequencies are significant ( $p\text{-value} < 0.05$ ) (Figure 4). For both  $\tau_{yw}$  and both catchments,  $F_{yw}$  decreases with decreasing sampling frequency from daily to weekly or bi-weekly. Changing the sampling frequency from weekly to bi-weekly has no consistent effect on the estimated mean  $F_{yw}$  among catchments. However,  $F_{yw}$  becomes highest when the

299 sampling frequency changes from sub-monthly (daily, weekly, or bi-weekly) to monthly in all  
 300 cases.



301  
 302 **Figure 4.** Effect of tracer data sampling frequency on the estimated  $F_{yw}$  using the proposed  
 303 procedure for (a, b) the Alp and (c, d) the Erlenbach catchments. The left panel (a, c) and right  
 304 panel (b, d) correspond to the age thresholds ( $\tau_{yw}$ ) of 2 and 3 months, respectively. The boxplots  
 305 show the uncertainty of the estimated  $F_{yw}$  values from the 100 best parameter sets. The  $p$ -value  
 306 indicates the significance levels when comparing the mean values between these groups. If no  $p$ -  
 307 value is given below two groups it indicates that their means are significantly different from each  
 308 other ( $p$ -value < 0.05).

309 To analyze the factors contributing to changes of  $F_{yw}$  with sampling frequency, we plot  
 310 (boxplot) the input data (precipitation, streamflow, and  $\delta^{18}\text{O}$ ), the parameters of the sine wave  
 311 function fitted to  $\delta^{18}\text{O}$  in precipitation ( $A_P$ ,  $\phi_P$ ,  $k_P$ ), as well as the parameters of the gamma TTD  
 312 ( $\alpha$  and  $\beta$ ) for each catchment (Alp, Erlenbach) and sampling frequency (daily, weekly, bi-  
 313 weekly, monthly) (Figure 5). It can be seen that extreme events might not be captured (Figure  
 314 5a-d) when the sampling frequency is reduced, but the spread (interquartile range) of the data  
 315 does not necessarily decrease (Figure 5a-d). The amplitude of the fitted sine wave to  $\delta^{18}\text{O}$  in  
 316 precipitation ( $A_P$ ) either increased or decreased with decreasing sampling frequency (Figure 4e)  
 317 and does not follow the pattern of  $F_{yw}$  (Fig. 4). Among the selected factors, only  $k_P$  (mean  $\delta^{18}\text{O}$

in precipitation) reflects the pattern found between  $F_{yw}$  and the sampling frequency (Fig. 5g). However, it is unclear how differences in  $k_p$  affect the differences in  $F_{yw}$  among different sampling frequencies.

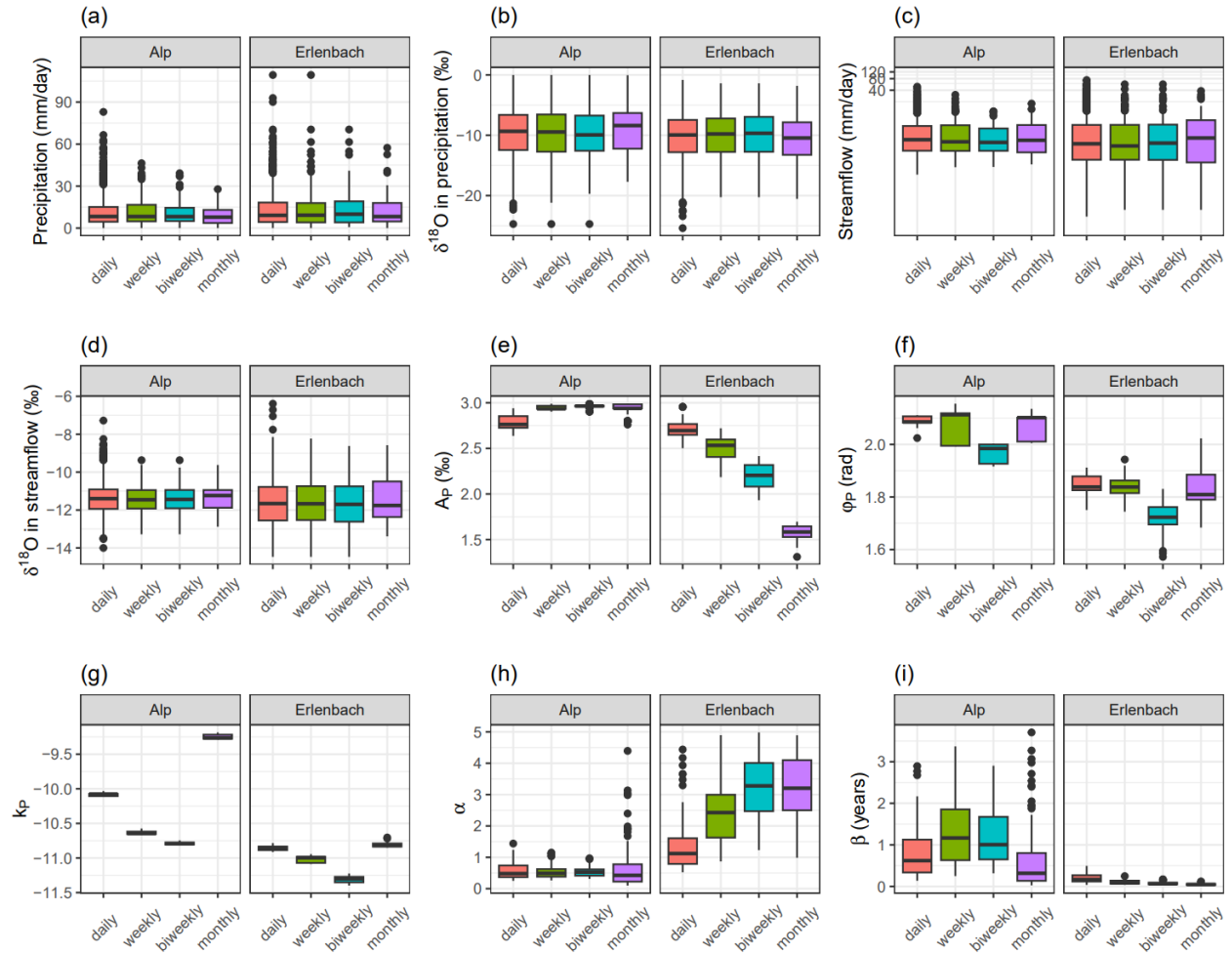


**Figure 5.** Boxplots of (a, b) precipitation amount and  $\delta^{18}O$  in precipitation, (c, d) streamflow amount and  $\delta^{18}O$  in streamflow, (e, f, g) parameters of the fitted sine wave to  $\delta^{18}O$  in precipitation, and (h, i) parameters of the gamma distribution from 100 best-fit runs for different sampling intervals (daily, weekly, bi-weekly, monthly) and catchments (Alp, Erlenbach).

## 4 Discussion

The proposed procedure for estimating  $F_{yw}$  uses the same assumptions as the traditional procedure. For example, the system is in a steady state, and tracer concentration in precipitation and streamflow follow the sine wave function (Kirchner, 2016). The advantages of the traditional method are that  $F_{yw}$  estimated from the amplitude ratio ( $A_s/A_p$ ) is free from aggregation bias. The proposed procedure is limited to the gamma TTD while the traditional procedure can be used to estimate  $F_{yw}$  even if the TTD is a non-gamma TTD as demonstrated in the virtual experiments by Kirchner (2016). In these virtual experiments, the tracer amplitude ratio from runoff of the combined catchment is approximately equal to the average  $F_{yw}$  from individual catchments (Figs. (11) and (13) in Kirchner (2016)). However, it is unclear what the age

thresholds corresponding to (1) the tracer amplitude ratio from runoff of the combined catchment and (2) the average  $F_{yw}$  from individual catchments are. For inter-catchment comparison using  $F_{yw}$ , it is necessary to know  $\tau_{yw}$ , therefore, parameters of the TTD. Nevertheless, practical applications of the traditional procedure often approximate  $F_{yw}$  using the amplitude ratio ( $F_{yw} \approx A_S/A_P$ ) without knowing the parameters of the TTD.

In this study, we showed that the estimated TTDs and  $F_{yw}$  from the traditional and the proposed procedure might largely differ. This is expected as we have a direct solution to find the (gamma) TTDs in the proposed procedure. In the traditional procedure, however, the TTDs are inferred from the sine waves fitted directly to  $\delta^{18}O$  in precipitation and streamflow. By doing this, the mass balance equation (Eq. 3) might not be hold, resulting error in the estimated TTDs.

Using the proposed procedure also allows us to evaluate the effects of data sampling frequency on the estimated young water fraction in a more precise way. Here, our results show that data sampling frequency could significantly affect the estimated  $F_{yw}$ , especially between sub-monthly and monthly sampling frequencies. Therefore, for inter-catchment comparison on  $F_{yw}$ , this effect should be accounted for if data of different frequencies are used. Here, we could not find which factor affects changes in  $F_{yw}$  with different sampling frequencies, suggesting that  $F_{yw}$  could vary from case to case (e.g., catchment, date of sample, sampling values).

The proposed procedure in this study also has some limitations. Our procedure for fitting (a) the sine wave to observed  $\delta^{18}O$  in precipitation and (b) the convolution of the input sine wave with the gamma distribution using a number of random parameter sets generated from LHS to the observed  $\delta^{18}O$  in streamflow are not computationally efficient and not robust when there are outliers in the data (which was not the case here). If this procedure is used, outliers should be removed from the data beforehand and more efficient nonlinear parameter estimation and optimization techniques (J. C. Nash, 2014) could be used. In addition, as the observed input and output  $\delta^{18}O$  data do not perfectly follow the sinusoidal function, various solutions exist (parameters of the sine wave and gamma distribution) that have similar goodness-of-fit (measured by the mean square error in this case). Furthermore, if users select too many simulations, the estimated  $F_{yw}$  could vary across the entire theoretical range [0,1], which is not a meaningful result. Therefore, one can further re-define behavioral simulations based on other measures for the goodness-of-fit, e.g., the Nash-Sutcliffe efficiency (NSE, Nash & Sutcliffe, 1970), the Kling-Gupta efficiency (KGE, Gupta et al., 2009), and R-square ( $R^2$ ), to select only a subset of simulations that will yield a meaningful estimate of  $F_{yw}$  while ensuring a sufficiently captured uncertainty in the estimated  $F_{yw}$ .

## 5 Conclusions

The young water fraction estimated from the seasonal tracer (isotope) cycles in precipitation and streamflow has been used in various inter-catchment comparison studies. However, the age thresholds associated with the estimated values of  $F_{yw}$  are often not given enough attention in such studies. Here, we proposed a more direct procedure, allowing the estimation of  $F_{yw}$  for any given age threshold. The proposed procedure is compared with the traditional procedure (Kirchner, 2016) and further used to evaluate the effects of data sampling

frequencies on the estimated  $F_{yw}$  using high-frequency tracer data in the Alp and its tributary catchment, the Erlenbach. We concluded that:

- The estimated  $F_{yw}$  can differ significantly between the traditional and proposed procedures.
- For inter-catchment comparison of  $F_{yw}$ ,  $\tau_{yw}$  should be fixed as changes in  $\tau_{yw}$  cause changes in the estimated  $F_{yw}$ .
- Tracer sampling frequency can the estimated  $F_{yw}$ .  $F_{yw}$  increases when the sampling frequency decreases from daily to bi-weekly time steps, but it increases when the sampling frequency is further decreased to monthly time steps.

Overall, the proposed procedure presented in this study facilitates an improved use of the young water fraction for inter-catchment comparison studies that aim at improving our understanding of the underlying hydrological processes controlling streamflow generation and instream water quality status.

## Acknowledgments

We thank Stefanie R. Lutz for her comments on the initial version of the manuscript.

## Open Research

The R package (Fyw) used in this work for estimating the young water fraction is available at <https://doi.org/10.5281/zenodo.7757959>. The results, including figures, in this study can be reproduced using the R Markdown document from <https://doi.org/10.5281/zenodo.8068420>. The isotope data used in this study can be downloaded from <https://www.doi.org/10.16904/envidat.242>.

## References

- Benettin, P., Fovet, O., & Li, L. (2020). Nitrate removal and young stream water fractions at the catchment scale. *Hydrological Processes*, 34(12). <https://doi.org/10.1002/hyp.13781>
- Benettin, P., Rodriguez, N. B., Sprenger, M., Kim, M., Klaus, J., Harman, C. J., van der Velde, Y., Hrachowitz, M., Botter, G., McGuire, K. J., Kirchner, J. W., Rinaldo, A., & McDonnell, J. J. (2022). Transit Time Estimation in Catchments: Recent Developments and Future Directions. In *Water Resources Research* (Vol. 58, Issue 11). <https://doi.org/10.1029/2022WR033096>
- Burt, E., Coayla Rimachi, D. H., Ccahuana Quispe, A. J., & West, A. J. (2022). Hydroclimate and bedrock permeability determine young water fractions in streamflow across the tropical Andes mountains and Amazon floodplain. *Hydrology and Earth System Sciences Discussions*, 2022, 1–27. <https://doi.org/10.5194/hess-2022-188>
- Gallart, F., Valiente, M., Llorens, P., Cayuela, C., Sprenger, M., & Latron, J. (2020). Investigating young water fractions in a small Mediterranean mountain catchment: Both precipitation forcing and sampling frequency matter. *Hydrological Processes*, 34(17). <https://doi.org/10.1002/hyp.13806>
- Gallart, F., von Freyberg, J., Valiente, M., Kirchner, J. W., Llorens, P., & Latron, J. (2020). Technical note: An improved discharge sensitivity metric for young water fractions. *Hydrology and Earth System Sciences*, 24(3). <https://doi.org/10.5194/hess-24-1101-2020>
- Gupta, H. V., Kling, H., Yilmaz, K. K., & Martinez, G. F. (2009). Decomposition of the mean squared error and NSE performance criteria: Implications for improving hydrological modelling. *Journal of Hydrology*, 377(1–2), 80–91. <https://doi.org/10.1016/j.jhydrol.2009.08.003>
- Hrachowitz, M., Benettin, P., van Breukelen, B. M., Fovet, O., Howden, N. J. K., Ruiz, L., van der Velde, Y., & Wade, A. J. (2016). Transit times-the link between hydrology and water quality at the catchment scale. *Wiley Interdisciplinary Reviews: Water*, 3(5), 629–657. <https://doi.org/10.1002/wat2.1155>
- Jasechko, S., Kirchner, J. W., Welker, J. M., & McDonnell, J. J. (2016). Substantial proportion of global streamflow less than three months old. *Nature Geoscience*, 9(2). <https://doi.org/10.1038/ngeo2636>
- Kirchner, J. W. (2016). Aggregation in environmental systems-Part 1: Seasonal tracer cycles quantify young water fractions, but not mean transit times, in spatially heterogeneous catchments. *Hydrology and Earth System Sciences*, 20(1). <https://doi.org/10.5194/hess-20-279-2016>
- Lutz, S. R., Krieg, R., Müller, C., Zink, M., Knöller, K., Samaniego, L., & Merz, R. (2018). Spatial Patterns of Water Age: Using Young Water Fractions to Improve the Characterization of Transit Times in Contrasting Catchments. *Water Resources Research*, 54(7), 4767–4784. <https://doi.org/10.1029/2017WR022216>
- McGuire, K. J., & McDonnell, J. J. (2006). A review and evaluation of catchment transit time modeling. *Journal of Hydrology*, 330(3–4), 543–563. <https://doi.org/10.1016/j.jhydrol.2006.04.020>

- Nash, J. C. (2014). On best practice optimization methods in R. *Journal of Statistical Software*, 60(2). <https://doi.org/10.18637/jss.v060.i02>
- Nash, J. E., & Sutcliffe, J. V. (1970). River flow forecasting through conceptual models part I - A discussion of principles. *Journal of Hydrology*, 10(3), 282–290. [https://doi.org/10.1016/0022-1694\(70\)90255-6](https://doi.org/10.1016/0022-1694(70)90255-6)
- Nguyen, T. V., Kumar, R., Lutz, S. R., Musolff, A., Yang, J., & Fleckenstein, J. H. (2021). Modeling Nitrate Export From a Mesoscale Catchment Using StorAge Selection Functions. *Water Resources Research*, 57(2), e2020WR028490. <https://doi.org/10.1029/2020wr028490>
- Nguyen, T. Van, Sarrazin, F. J., Ebeling, P., Musolff, A., Fleckenstein, J., & Kumar, R. (2022). Towards understanding of long-term nitrogen transport and retention dynamics across German catchments. <https://doi.org/10.1002/essoar.10511836.1>
- R Core Team. (2021). R core team (2021). In *R: A language and environment for statistical computing*. R Foundation for Statistical Computing, Vienna, Austria. URL <http://www.R-project.org>.
- Song, C., Wang, G., Liu, G., Mao, T., Sun, X., & Chen, X. (2017). Stable isotope variations of precipitation and streamflow reveal the young water fraction of a permafrost watershed. *Hydrological Processes*, 31(4). <https://doi.org/10.1002/hyp.11077>
- Staudinger, M., Stoelzle, M., Seeger, S., Seibert, J., Weiler, M., & Stahl, K. (2017). Catchment water storage variation with elevation. *Hydrological Processes*, 31(11). <https://doi.org/10.1002/hyp.11158>
- Stockinger, M. P., Bogen, H. R., Lücke, A., Diekkrüger, B., Cornelissen, T., & Vereecken, H. (2016). Tracer sampling frequency influences estimates of young water fraction and streamwater transit time distribution. *Journal of Hydrology*, 541. <https://doi.org/10.1016/j.jhydrol.2016.08.007>
- Su, X., Yan, X., & Tsai, C. L. (2012). Linear regression. *Wiley Interdisciplinary Reviews: Computational Statistics*, 4(3). <https://doi.org/10.1002/wics.1198>
- von Freyberg, J., Allen, S. T., Seeger, S., Weiler, M., & Kirchner, J. W. (2018). Sensitivity of young water fractions to hydro-climatic forcing and landscape properties across 22 Swiss catchments. *Hydrology and Earth System Sciences*, 22(7). <https://doi.org/10.5194/hess-22-3841-2018>
- von Freyberg, J., Rücker, A., Zappa, M., Schlumpf, A., Studer, B., & Kirchner, J. W. (2022). Four years of daily stable water isotope data in stream water and precipitation from three Swiss catchments. *Scientific Data*, 9(1). <https://doi.org/10.1038/s41597-022-01148-1>